Supporting Information

Molecular brush-based ultrathin polymer electrolytes with stable interfaces for high-voltage large-areal-capacity lithium metal batteries

Rongfeng Liao, Congping Li, Minghong Zhou, Ruliang Liu, Shaohong Liu,* and Dingcai Wu*

Experimental section

Synthesis of (2-oxo-1,3-dioxolan-4-yl) methyl methacrylate (CCMA)

CCMA was synthesized according to the reported procedures.[1] 13 mL of 4-hydroxymethyl-1,3-dioxolan-one, 22 mL of trimethylamine and 100 mL of methylene chloride were added into a three-neck flask and purged with N_2. Subsequently, 15 mL of methacryloyl chloride diluted with 30 mL methylene chloride was added dropwise for 1 h under an ice bath. The reaction was kept under stirring at room temperature for 12 h. Finally, a faint yellow liquid was obtained by extraction and rotary evaporation.

Synthesis of BC-*g*-P(CCMA-*co*-TFEMA)

BC-Br was first synthesized according to the reported procedures.[2] Then, 200 mg of BC-Br was added into Schlenk flask containing 13.9 mg of copper(II) bromide ($CuBr_2$), 130 μL of N,N,N′,N″,N‴-pentamethyldiethylenetriamine (PMDETA), 2 mL of CCMA, 4 mL of 2,2,2-trifluoroethyl methacrylate (TFEMA, purified by a basic alumina column) and 8 mL of N,N-dimethylformamide (DMF). After bubbling N_2 for 1 h and injecting 140 mg of ascorbic acid in 1 mL of DMF, the flask was immersed in an oil bath at 80 ºC for 24 h under stirring, followed by exposing to air to stop the reaction. The as-obtained BC-*g*-P(CCMA-*co*-TFEMA) was then centrifuged and washed with DMF.

BC-*g*-PCCMA and BC-*g*-PTFEMA were synthesized according to similar procedures to BC-*g*-P(CCMA-*co*-TFEMA), in which 6 mL of CCMA or TFEMA was used instead of 2 mL of CCMA and 4 mL of TFEMA. The conventional linear polymer P(CCMA-*co*-TFEMA) was synthesized according to similar procedures to BC-*g*-P(CCMA-*co*-TFEMA), in which 50 μL of ethyl 2-bromoisobutyrate (EBiB) was used instead of 200 mg of BC-Br.

Preparation of BPCT-PE

BC-*g*-P(CCMA-*co*-TFEMA) membrane was first obtained via vacuum filtrating dispersions of BC-*g*-P(CCMA-*co*-TFEMA) molecular brushes in DMF. Then, BPCT-PE was obtained by swelling the BC-*g*-P(CCMA-*co*-TFEMA) membrane in liquid electrolyte (1.0 M $LiPF_6$ in ethylene carbonate/diethyl carbonate (1/1, v/v) with 5% fluoroethylene carbonate as additive). The content of liquid electrolyte in BPCT-PE was 55 wt.%.

BPC-PE and BPT-PE were obtained in the same way with BC-*g*-PCCMA and BC-*g*-PTFEMA as the building blocks, respectively. For B/PCT-PE, BC/P(CCMA-*co*-TFEMA) membrane was obtained by casting the homogeneous mixture of linear polymer P(CCMA-*co*-TFEMA) and BC in DMF on polyfluortetraethylene plate, followed by heating at 60 ºC for 12 h.

Material characterization

Fourier transform infrared (FTIR) spectra were obtained based on a FTIR spectroscope (Nicolet iS50, Thermo Fisher Scientific). Morphologies and elemental mappings of samples were investigated by a field emission scanning electron microscope (S-4800, Hitachi). Thicknesses of membranes were measured by a digital display micrometer thickness gauge. Thermogravimetric analysis (TGA) measurements were conducted on a thermogravimetric analyzer (TG 209 F1 Libra, Netzsch) in the temperature range from 30 to 800 ºC with a heating rate of 10 ºC min^{-1} under nitrogen atmosphere. The molecular weight was analyzed by a gel permeation chromatography (Breeze GPC, Waters). Atomic force microscopy (AFM) was carried out on an atomic force microscope (Dimension Fastscan, Bruker) in peak force quantitative nanomechanics mode and Young's moduli were analyzed using the Derjaguin-Muller-Toporov model. The elasticity moduli of membranes were measured using a dynamic ultra-micro hardness tester (DUH-W201S, Shimadzu) with 0.20 mN preset test force. ^{7}Li nuclear magnetic resonance (^{7}Li NMR) experiment was performed on an NMR spectrometer (Ascend 400 MHz, Bruker). The Raman spectra were obtained on a micro-Raman spectrometer (inVia Qontor, Renishaw) using a 785-nm-wavelength laser. The TEM images were obtained using a transmission electron microscope (Tecnai G2

F30, FEI). X-ray photoelectron spectroscopy (XPS) was performed on an X-ray photoelectron spectrometer (K-Alpha, Thermo Fisher Scientific).

Electrochemical measurements

CR2032 coin cells were assembled to perform all electrochemical measurements. Ionic conductivity (σ) was evaluated in the frequency range from 0.1 to 10^6 Hz at various temperatures from 30 to 90 °C by electrochemical impedance spectroscopy (EIS) measurement using an electrochemical station (CHI660E, Chenhua).

The σ was calculated according to equation (1):

$$\sigma = \frac{L}{SR} \quad (1)$$

where L is the thickness of membrane; S is the cross-section area of the electrode; R is the bulk resistance obtained from the EIS measurement.

The lithium ion transference number (t_{Li^+}) was calculated according to Bruce-Vincent equation (2):

$$t_{\mathrm{Li}^+} = \frac{I_S(\Delta V - I_0 R_0)}{I_0(\Delta V - I_S R_S)} \quad (2)$$

where ΔV is the constant polarization voltage applied (10 mV); I_0 and R_0 are the initial state current and resistance, respectively; I_s and R_s are the steady state current and resistance, respectively.

Electrochemical stability window of various electrolytes was measured by linear sweep voltammetry (LSV) with the cell configuration of Li/stainless-steel at a scan rate of 5 mV s^{-1} over 1~6 V. Li/Li symmetric cells were assembled with Li foils (thickness = 450 μm) as the working electrode and counter electrode, respectively. Li/Li symmetric cells were activated for 5 cycles at 0.1 mA cm^{-2} and 0.1 mA h cm^{-2} before the cycling tests. For Li/$LiFePO_4$ cells, the cathode was prepared by mixing the $LiFePO_4$, Super P, and PVDF (8:1:1 by weight) in NMP solvent under vigorous stirring. The obtained slurry was cast onto Al foil followed by drying in a vacuum oven at 60 °C for 24 h. The mass loading of $LiFePO_4$ was about 2.2 mg cm^{-2}. The rate and cycling performances of Li/$LiFePO_4$ cells were conducted between 2 and 4 V at 30 °C (1C = 170 mA h g^{-1}). Li/$LiFePO_4$ cells were activated for 3 cycles at 0.1C before the cycling tests. Li/NCM811 cells were charged at 0.2C and discharged at 1C at 30 °C between

3.0 and 4.3/4.5 V (1C = 188 mA h g^{-1}) and were activated for 3 cycles at 0.1C before the cycling test.

Molecular dynamics simulations

The coordination structures of solvents, cations and anions in different electrolytes were simulated by molecular dynamics (MD) simulation with GROMACS 2021 software package. The OPLS-AA force field and Auxiliary Tools of Force Field were used to parametrize all atoms. Chemical compositions of simulation systems for LE and BPCT-PE were in accordance with experimental results. In the simulation system for LE, 100 $LiPF_6$, 713 EC, 392 DEC and 69 FEC molecules were added to a cube box. In the simulation system for BPCT-PE, 100 $LiPF_6$, 713 EC, 392 DEC, 69 FEC, 6 PCCMA and 18 PTFEMA molecules were added to a cube box; the polymerization degrees of PCCMA and PTFEMA were set at 10. The steepest descent method was applied to minimize the initial energy for each system with a force tolerance of 1 kJ mol^{-1} nm^{-1} and a maximum step size of 0.002 ps before MD calculations. The MD simulation was processed in an NPT ensemble and the simulation time was 20 ns. In NPT simulations, the pressure was maintained at 1 bar by the Berendsen barostat in an isotropic manner and the temperature was maintained by the V-rescale thermostat at 298.15 K. The Particle-Mesh-Ewald with a fourth-order interpolation was used to evaluate the electrostatic interactions; whereas a cutoff of 1.0 nm was employed to calculate the short-range van der Waals interactions.

Density functional theory calculations

The binding energy of Li^+ with PCCMA, PTFEMA, EC, DEC, FEC or PF_6^- in BPCT-PE was carried out with the Gaussian 16 program. The B3LYP functional was adopted for all calculations in combination with Becke-Johnson damping (DFT-D3BJ). For geometry optimization and frequency calculations, the 6-31G(d,p) basis set was used and the optimal geometry for each compound was determined. The singlet point energy calculations were performed with 6-311G(d,p) basis set, and the Solvation Model Density implicit solvation model was used to account for the solvation effect of EC/DEC/FEC=19:19:2 (volume ratio). The binding energy (E_b) of Li^+ with PCCMA, PTFEMA, EC, DEC, FEC or PF_6^- was calculated by equation (3):

$$E_{\mathrm{b}} = E_{\mathrm{total}} - E_{\mathrm{Li+}} - E_{\mathrm{M}} \quad (3)$$

where E_{total} and $E_{\mathrm{Li+}}$ are the total energy of the Li^+-M complex and the energy of Li^+, respectively; E_{M} is the energy of PCCMA, PTFEMA, EC, DEC, FEC or PF_6^-.

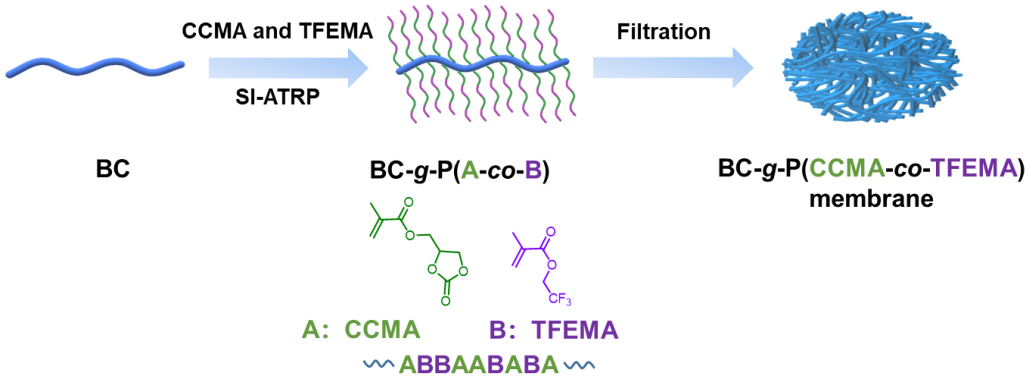

Fig. S1 Preparation procedures of BC-*g*-P(CCMA-*co*-TFEMA) membrane.

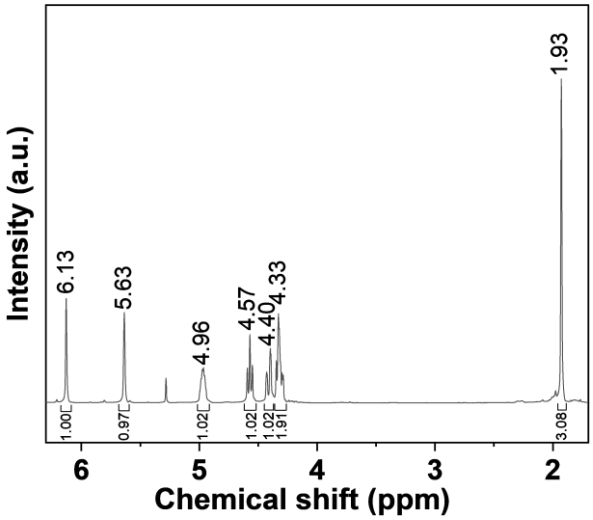

Fig. S2 ^{1}H NMR spectrum of CCMA monomer in $CDCl_3$ (400 MHz): δ 6.13 (s, 1H), 5.63 (s, 1H), 4.96 (m, 1H), 4.57 (t, 1H), 4.40 (m, 1H), 4.33 (m, 2H), and 1.93 (s, 3H).

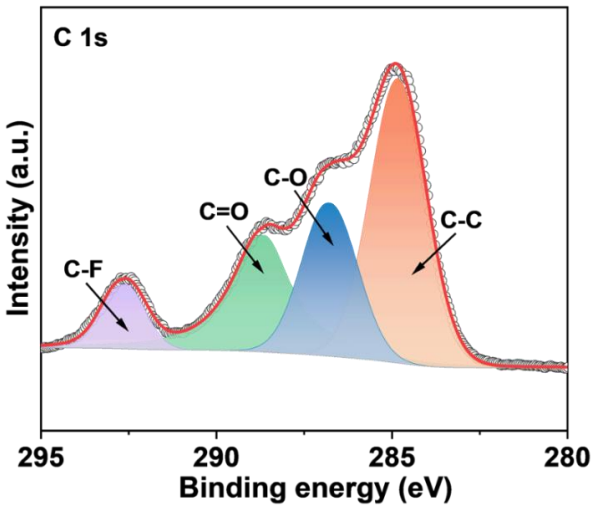

Fig. S3 High-resolution C 1s XPS spectrum of BC-*g*-P(CCMA-*co*-TFEMA).

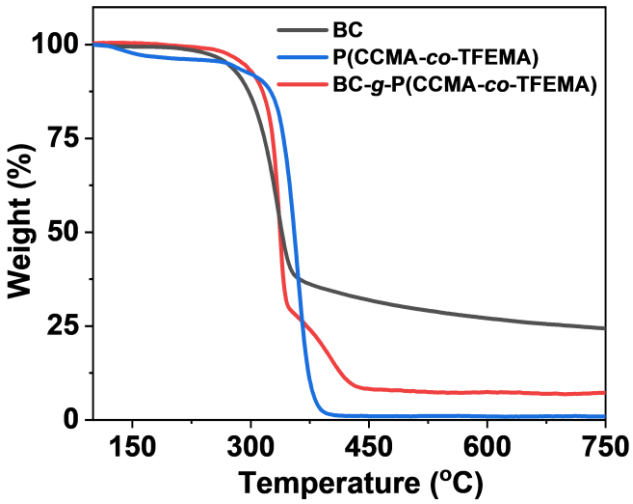

Fig. S4 Thermogravimetric curves of BC, P(CCMA-*co*-TFEMA) and BC-*g*-P(CCMA-*co*-TFEMA).

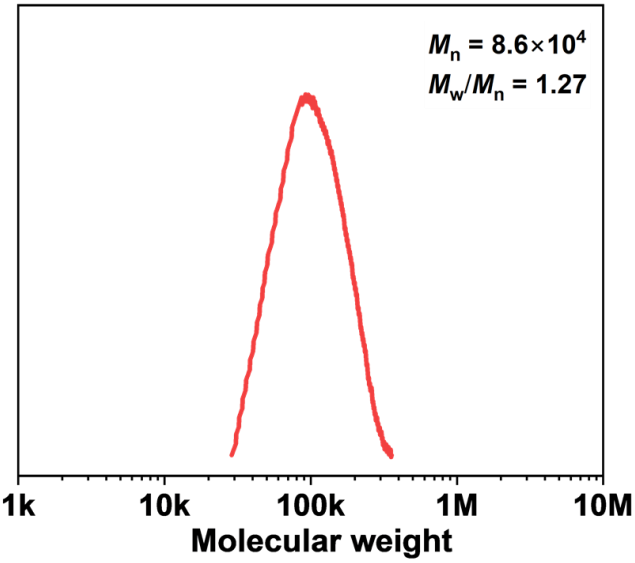

Fig. S5 GPC curve of free polymer P(CCMA-*co*-TFEMA).

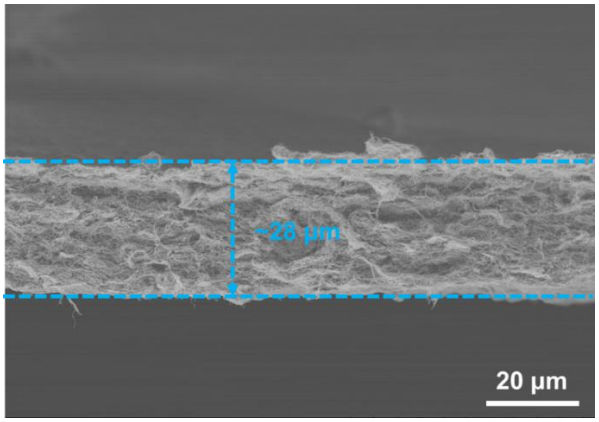

Fig. S6 Cross-section SEM image of BC-*g*-P(CCMA-*co*-TFEMA) membrane.

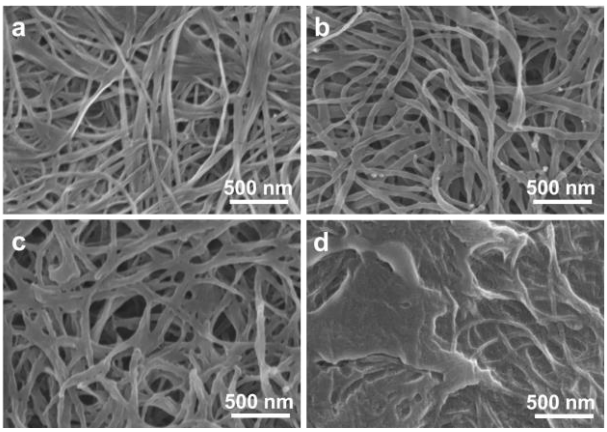

Fig. S7 SEM images of (a) BC, (b) BC-*g*-PCCMA, (c) BC-*g*-PTFEMA and (d) BC/P(CCMA-*co*-TFEMA) membranes.

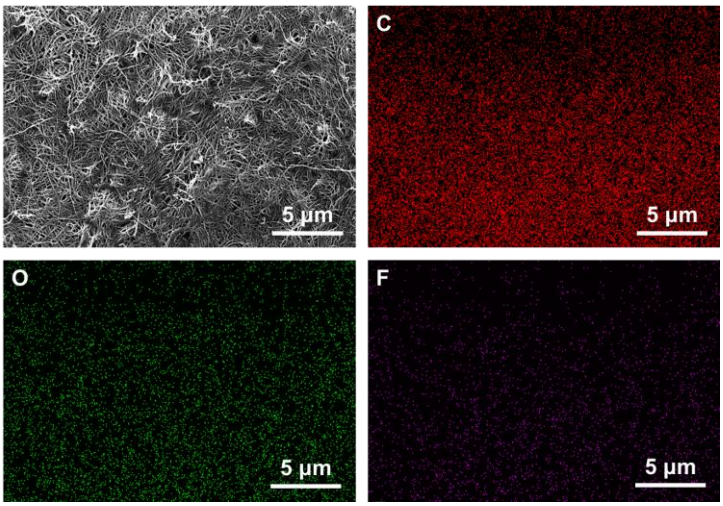

Fig. S8 SEM image and corresponding elemental mapping images of carbon, oxygen and fluorine for BC-*g*-P(CCMA-*co*-TFEMA) membrane.

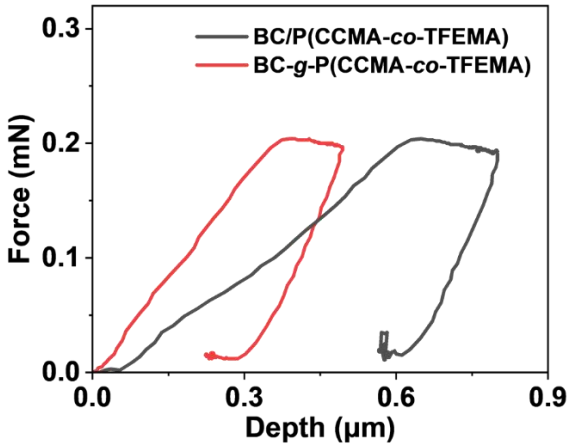

Fig. S9 Force-depth curves of BC/P(CCMA-*co*-TFEMA) and BC-*g*-P(CCMA-*co*-TFEMA) membranes under the same maximum force (0.2 mN).

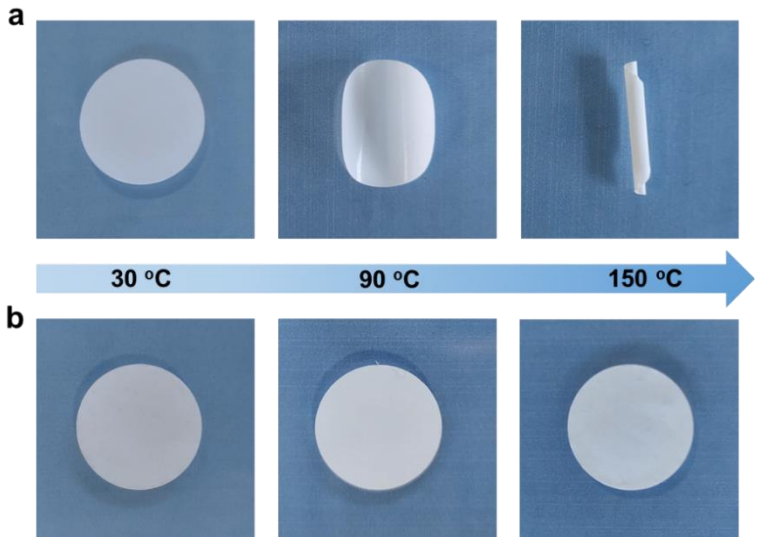

Fig. S10 Thermal shrinkage of (a) PP separator and (b) BC-*g*-P(CCMA-*co*-TFEMA) membrane after heating at different temperatures for 0.5 h.

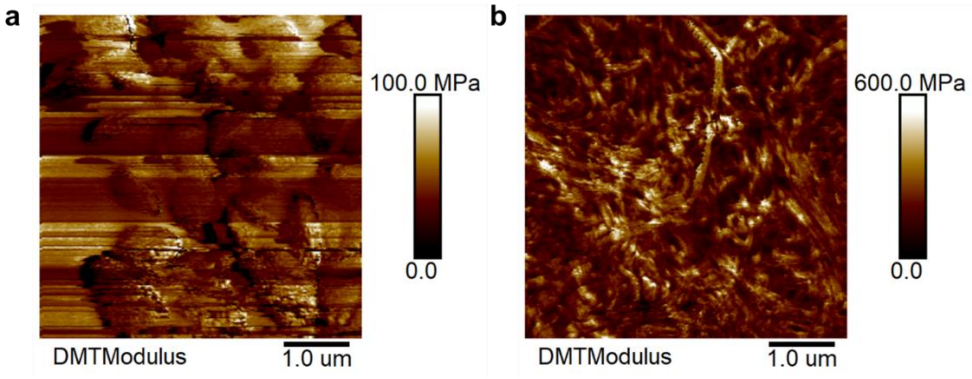

Fig. S11 AFM Young's modulus mappings of (a) B/PCT-PE and (b) BPCT-PE.

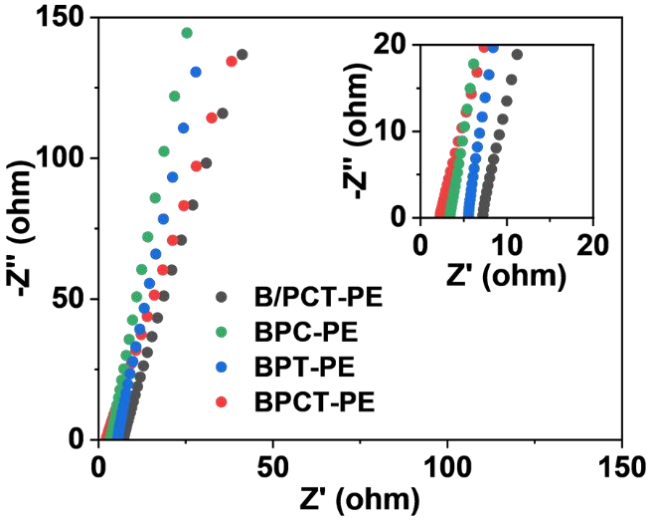

Fig. S12 Nyquist plots of B/PCT-PE, BPC-PE, BPT-PE and BPCT-PE at 30 °C.

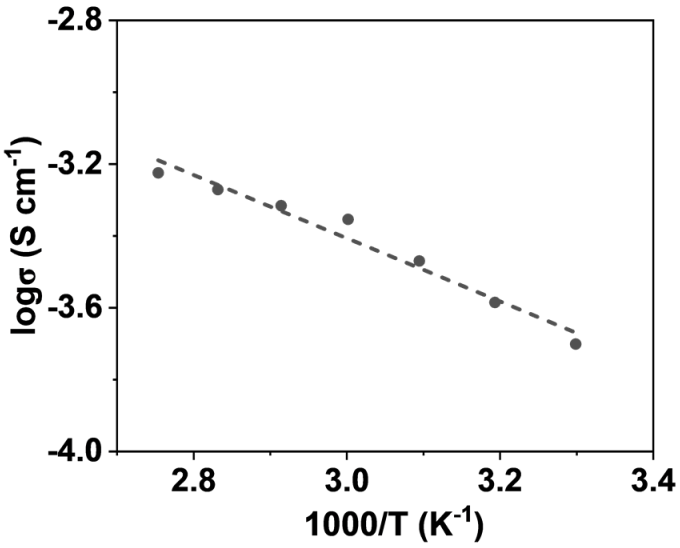

Fig. S13 Ionic conductivity fitted by Arrhenius plots for B/PCT-PE.

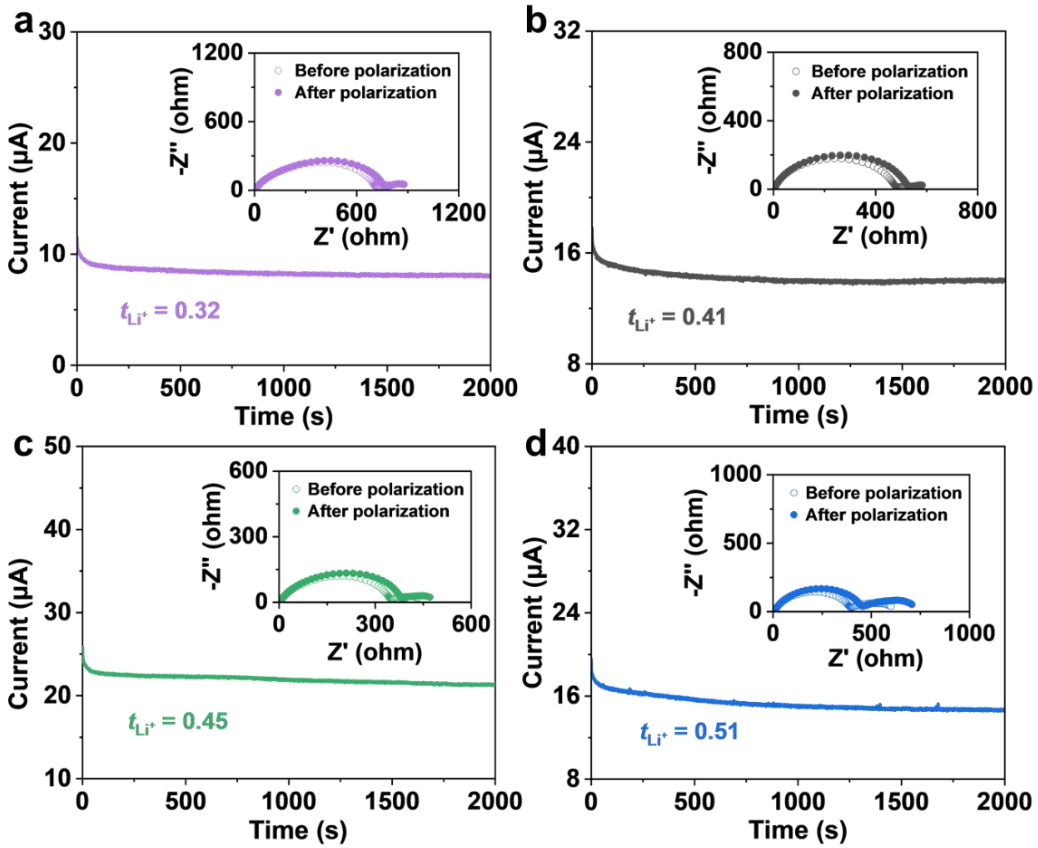

Fig. S14 Chronoamperometry profiles of Li/Li symmetric cells with (a) BC/LE, (b) B/PCT-PE, (c) BPC-PE and (d) BPT-PE under a polarization voltage of 10 mV, and their corresponding EIS curves before and after polarization (inset).

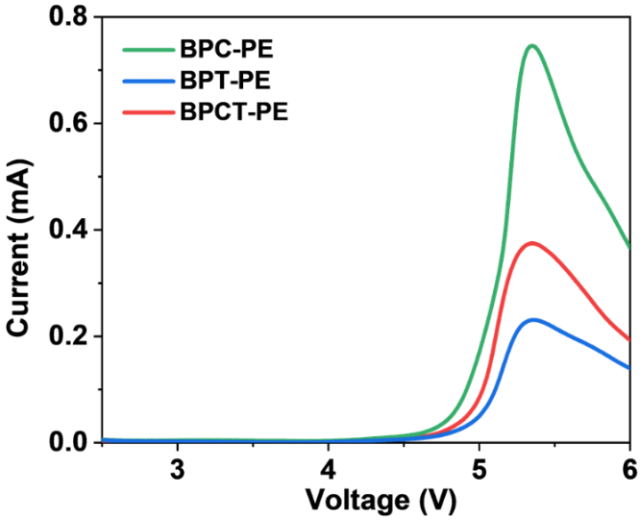

Fig. S15 LSV curves for BPC-PE, BPT-PE and BPCT-PE at a scan rate of 5 mV s^{-1}.

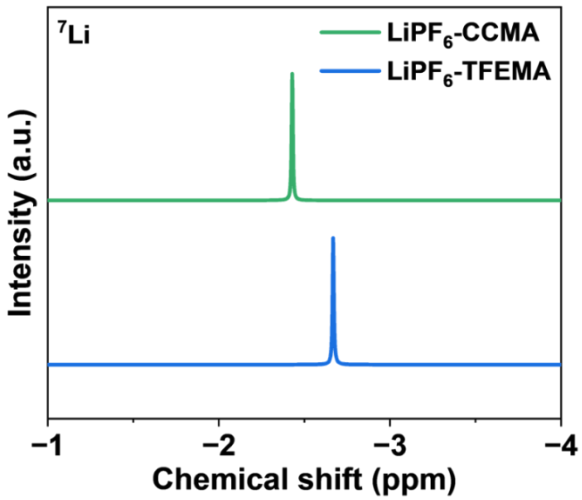

Fig. S16 ^{7}Li NMR spectra of $LiPF_6$-CCMA and $LiPF_6$-TFEMA in CD_3CN.

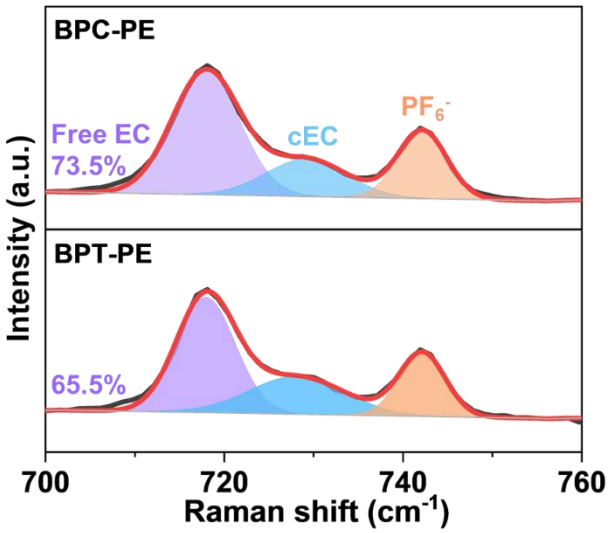

Fig. S17 Raman spectra of BPC-PE and BPT-PE.

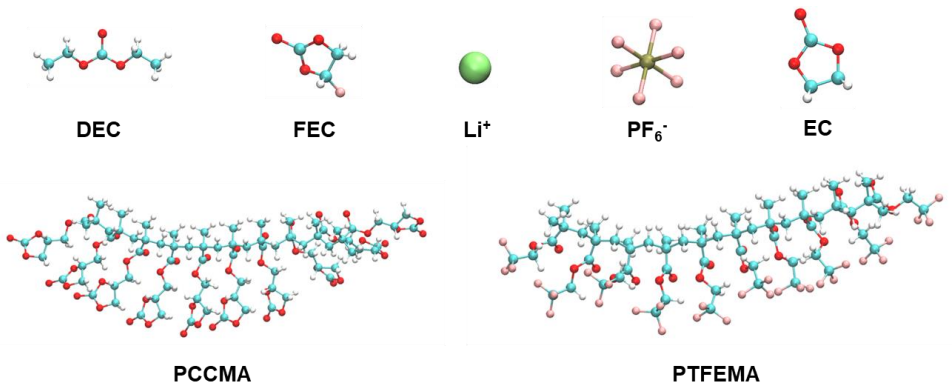

Fig. S18 Molecular configurations of the components used in MD simulation.

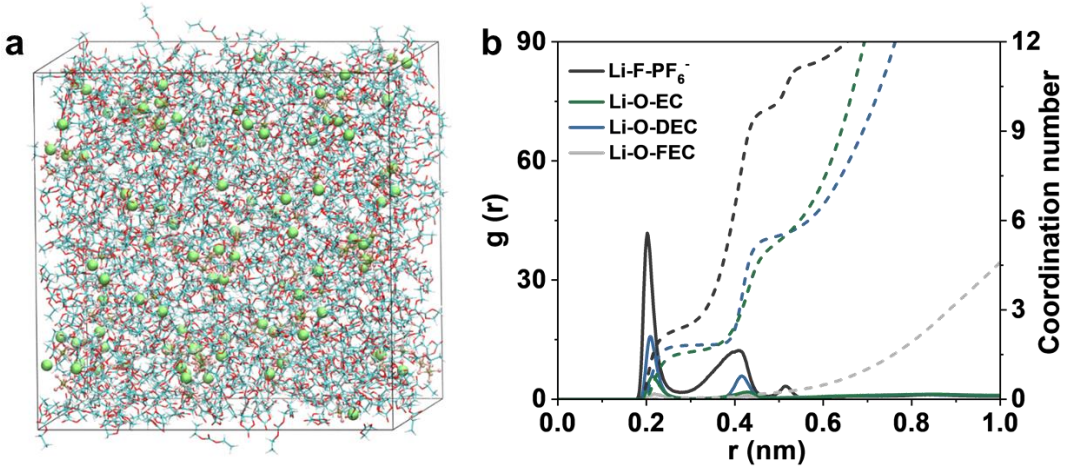

Fig. S19 (a) A snapshot of the MD simulation box for LE. (b) Radial distribution functions (solid lines) and corresponding coordination numbers (dashed lines) of LE.

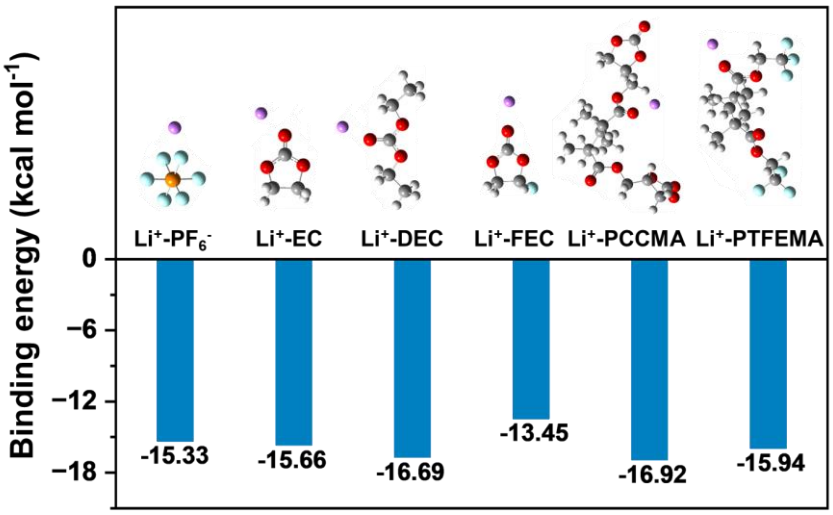

Fig. S20 DFT-calculated binding energy of Li^+ with PF_6^-, EC, DEC, FEC, PCCMA or PTFEMA.

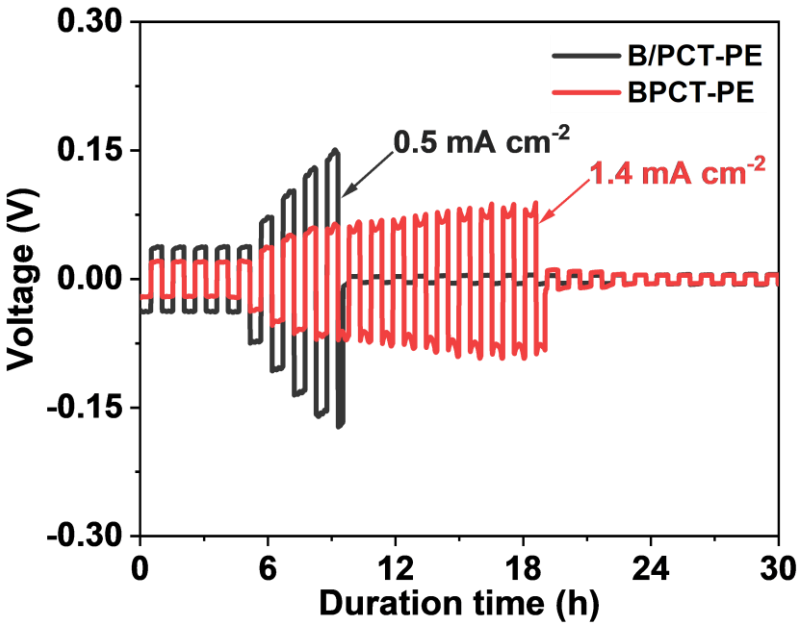

Fig. S21 Voltage-time profiles for critical current density tests of Li/Li symmetric cells with B/PCT-PE and BPCT-PE.

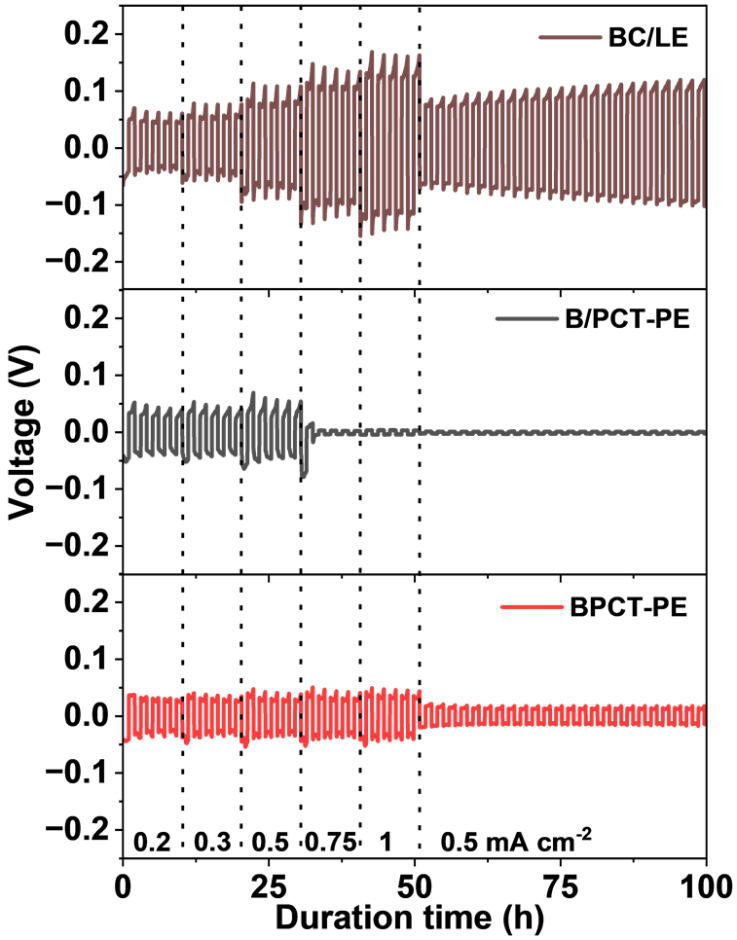

Fig. S22 Rate performance of Li/Li symmetric cells with BC/LE, B/PCT-PE and BPCT-PE at various current densities.

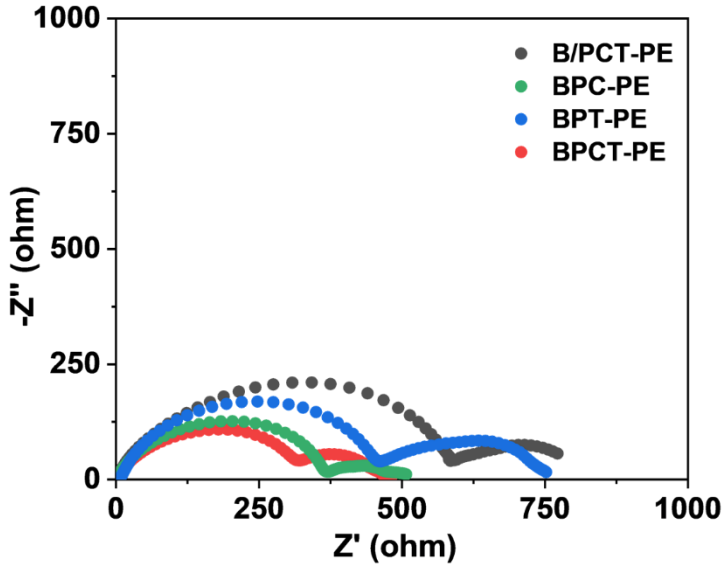

Fig. S23 Nyquist plots of Li/Li symmetric cells with B/PCT-PE, BPC-PE, BPT-PE and BPCT-PE.

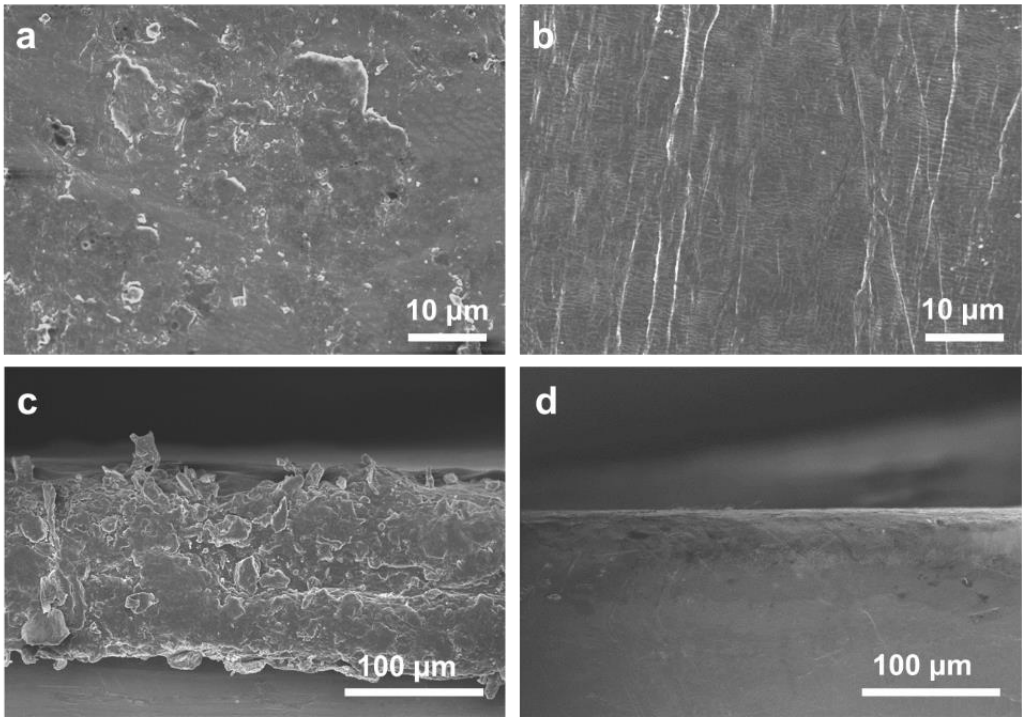

Fig. S24 (a, b) Top-view and (c, d) cross-section SEM images of lithium metal assembled with (a, c) BPC-PE and (b, d) BPCT-PE after lithium plating/stripping at 0.1 mA cm^{-2} and 0.1 mA h cm^{-2} for 100 cycles.

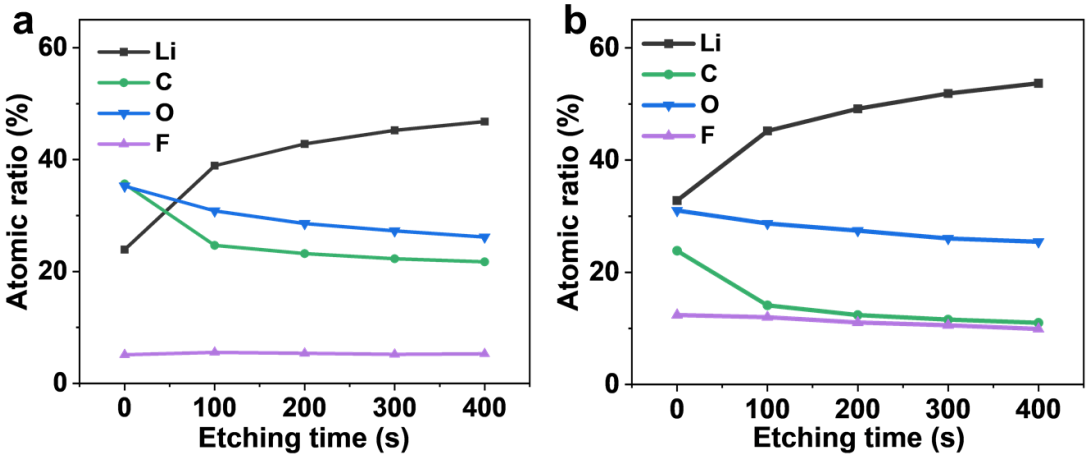

Fig. S25 Atomic composition ratios of C, Li, O and F by XPS depth measurement of the SEI formed in (a) BPC-PE and (b) BPCT-PE at 0.1 mA cm^{-2} and 0.1 mA h cm^{-2} after 100 cycles.

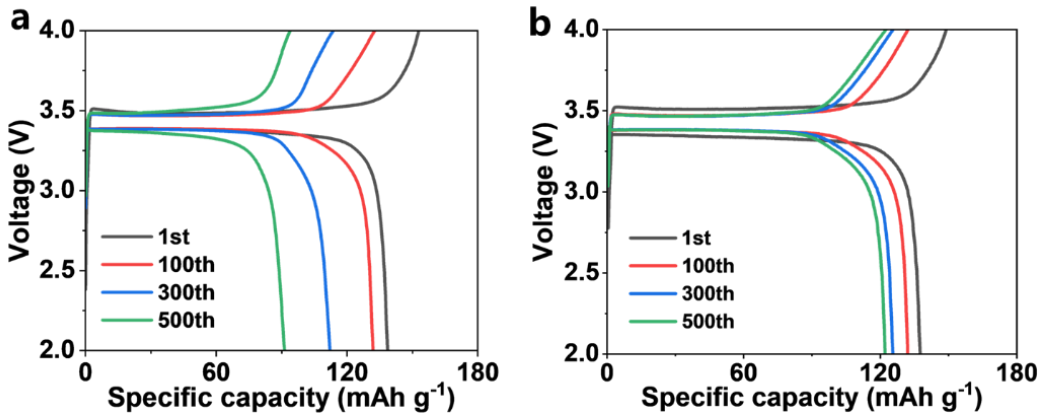

Fig. S26 Charge-discharge profiles of Li/$LiFePO_4$ cells with (a) PP/LE and (b) BPCT-PE at 1C.

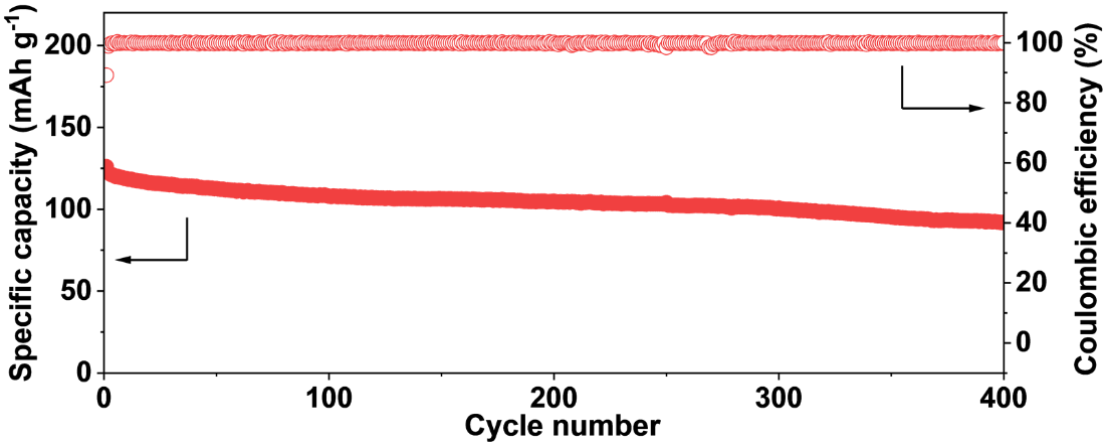

Fig. S27 Cycling performance of Li/$LiFePO_4$ cell with BPCT-PE at 2C.

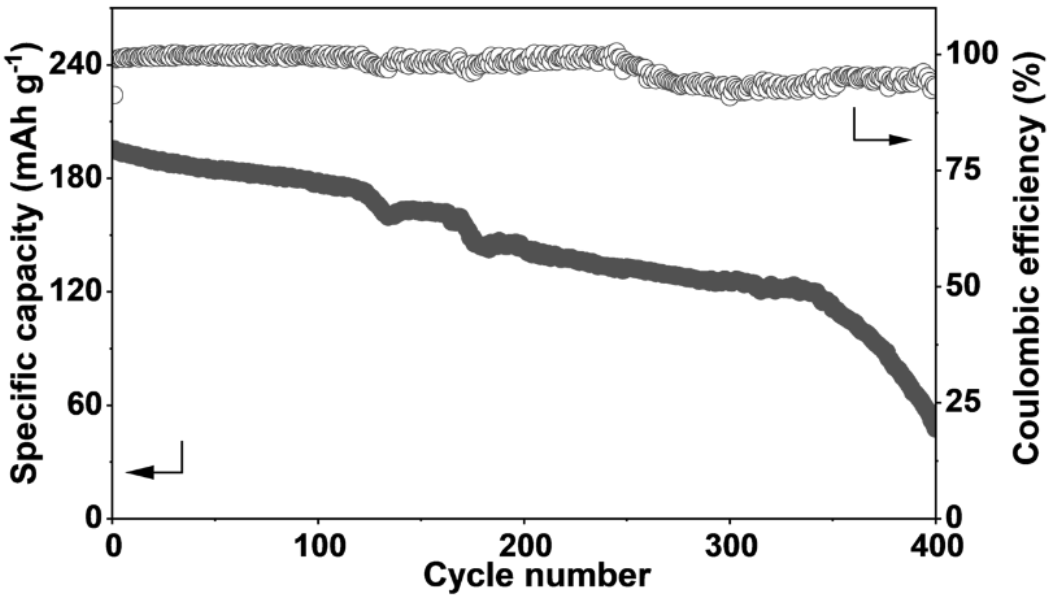

Fig. S28 Cycling performance of Li/NCM811 cell with PP/LE at charging/discharging rates of 0.2/1C with mass loading of 7.5 mg cm^{-2} at 4.3 V.

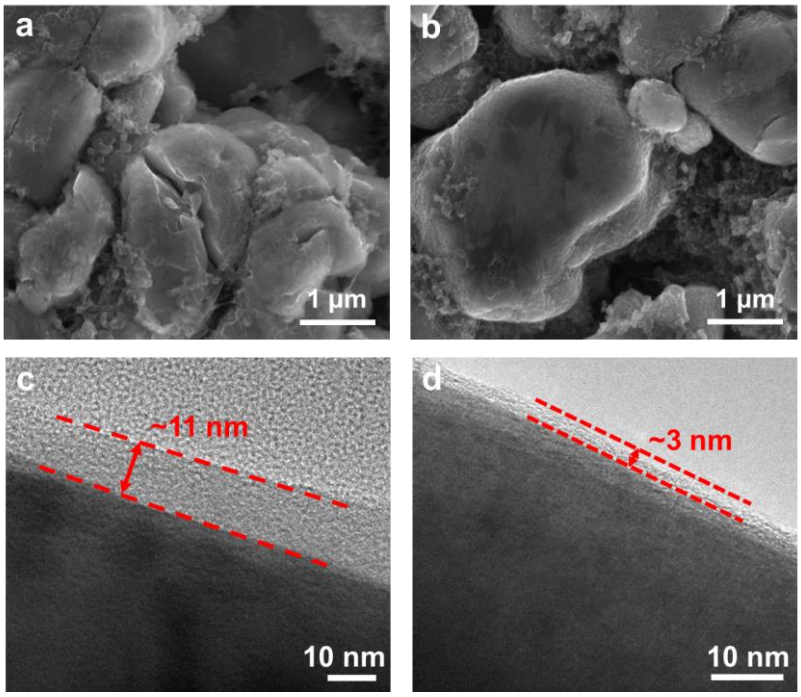

Fig. S29 SEM and TEM images of NCM811 cathodes with (a, c) PP/LE and (b, d) BPCT-PE after 50 cycles.

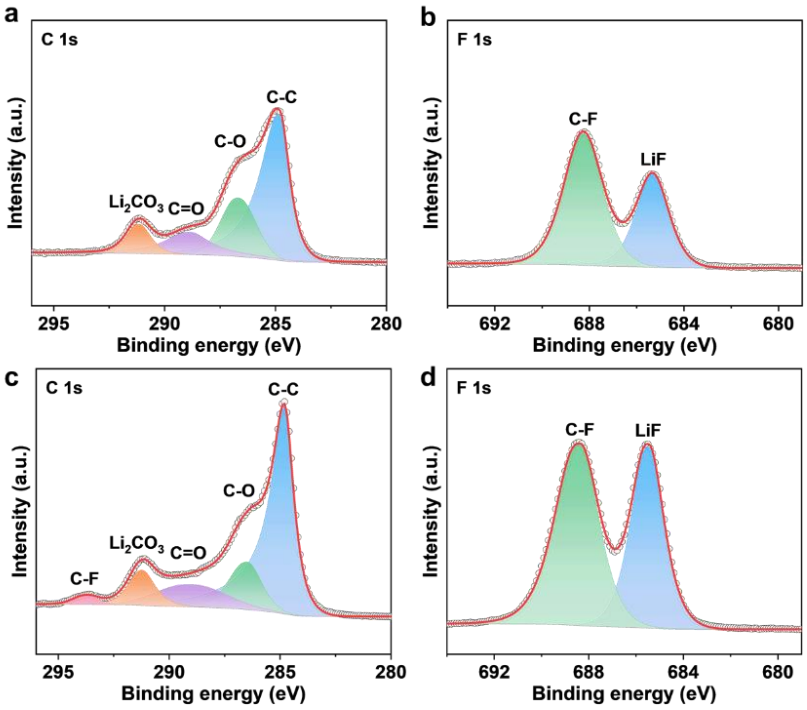

Fig. S30 High-resolution C 1s and F 1s XPS spectra of NCM811 cathodes with (a, b) PP/LE and (c, d) BPCT-PE after 50 cycles.

Table S1. Thickness of reported solid-state electrolytes.

Sample	Thickness (μm)	Type	Reference
PU-EO_{12}/LiTFSI/$TEG_{41\%}$	400~500	PE	3
FPH-Li	45	PE	4
PVEC-PE	125	PE	5
ANP-5	80~100	PE	6
PS-3H4S	30	PE	7
PTADOL SPE	7.2	PE	8
PVDF/DEE-1:10	500	PE	9
SIGPE	170	PE	10
DLPE	100	PE	11
DSICE	12	PE	12
PISSE	320	PE	13
P(VDF-TrFE-CTFE)	70	PE	14
FEC-SPE	300~400	PE	15
MIC	80	PE	16
PVDF-HFP/LiTFSI/G4	56	PE	17
LPO@LLZTO	500	IE	18
LLTO	41	IE	19
LATP	70	IE	20
LAGP	100	IE	21
$Li_{10}GeP_2S_{12}$	1000	IE	22
Ag-C/LLZTO	74	IE	23
LLCZN@LAO	1000	IE	24
Li_3PS_4-2$LiBH_4$	600	IE	25
Li_3InCl_6	320	IE	26
Li_6PS_5Cl	35	IE	27
Trilayer CPE w/ Porous Scaffold	150	CE	28
LOCB/NBR CPE	310	CE	29
NCSE-VA	46.18	CE	30
CSPE	200	CE	31
PV-CPE	100~300	CE	32
PEO-10%CeO_2	150	CE	33
PEO-$NH_3^+ \cdot SO_3^-$@ZIFs	113.56	CE	34
Co_3O_4@PDA CPE	100	CE	35
PEO/ZIF-67	73	CE	36
PEO/PVDF/LLZTO	200	CE	37
UIO-66/PAN/PEO/LiTFSI	100	CE	38
NCN-CPE	200	CE	39
ES-CSE	135	CE	40
PVBL	67	CE	41
PTFE/LLZTO/SN	100	CE	42
PEO/PEG-3LGPS	48	CE	43

Table S2. Cycling performance comparison between Li/$LiFePO_4$ cells with BPCT-PE and those with reported solid-state electrolytes.

Sample	Rate	Cycle number	Capacity retention	Reference
BPCT-PE	**1C**	**1000**	**83%**	**This work**
PTADOL SPE	0.5C	300	85.6%	8
PVDF/DEE-1:10	1C	650	80%	9
HGPE/TpPa-2	0.5C	1000	75%	44
PDOL@PDA/PVDF-HFP	1C	200	87.13%	45
BSPE	0.5C	1000	80%	46
PETPTA/LLZTO	0.1C	100	82.3%	47
PEGGPE@HT	1C	400	96.4%	48
LLZO/PMMA/PEGDA	1C	300	90.4%	49

Table S3. Cycling performance comparison between Li/NCM811 cells with BPCT-PE and those with reported solid-state electrolytes.

Sample	Type	Cycle number	Areal capacity (mA h cm^{-2})	Cut-off voltage (V)	Reference
BPCT-PE	**PE**	**400**	**1.53**	**4.5**	**This work**
	PE	**600**	**1.44**	**4.3**	
BSPE	PE	55	0.53	4.2	46
PEGGPE@HT	PE	200	0.42	4.5	48
PTADOL SPE	PE	150	0.58	4.3	8
MDPE	PE	150	0.85	4.3	50
FPCSPE	PE	300	0.28	4.5	51
P(IL-OFHDODA-VEC)	PE	200	0.12	4.5	52
Li-NC/PVDF	PE	700	0.18	4.3	53
P(LiMTFSI)-SANPE	PE	55	0.18	4.2	54
LNO/DMAA GPE	PE	400	0.31	4.3	55
SiO_2/ZSM-5/PVDF-HFP	CE	300	0.86	4.3	56
QDL-CPEs	CE	100	0.45	4.2	57
LLZO-Ga/PVDF-HFP	CE	360	0.64	4.3	58
LLZO/PMMA/PEGDA	CE	200	0.21	4.3	49
PVDF/Cellulose/B_2O_3	CE	200	0.21	4.2	59
POSS-NH_2/PDOL	CE	100	0.30	4.3	60
PDL@LLZTO	CE	500	0.37	4.5	61

References

1 E. R. Beckel, J. W. Stansbury and C. N. Bowman, *Macromolecules*, 2005, **38**, 9474-9481.

2 M. Zhou, R. Liu, D. Jia, Y. Cui, Q. Liu, S. Liu and D. Wu, *Adv. Mater.*, 2021, **33**, 2100943.

3 Y. Guo, X. Qu, Z. Hu, J. Zhu, W. Niu and X. Liu, *J. Mater. Chem. A*, 2021, **9**, 13597-13607.

4 P. Zhai, Z. Yang, Y. Wei, X. Guo and Y. Gong, *Adv. Energy Mater.*, 2022, **12**, 2200967.

5 Z. Lin, X. Guo, Z. Wang, B. Wang, S. He, L. A. O'Dell, J. Huang, H. Li, H. Yu and L. Chen, *Nano Energy*, 2020, **73**, 104786.

6 D. M. Shin, J. E. Bachman, M. K. Taylor, J. Kamcev, J. G. Park, M. E. Ziebel, E. Velasquez, N. N. Jarenwattananon, G. K. Sethi, Y. Cui and J. R. Long, *Adv. Mater.*, 2020, **32**, 1905771.

7 R. Y. Wang, S. Jeong, H. Ham, J. Kim, H. Lee, C. Y. Son and M. J. Park, *Adv. Mater.*, 2022, **35**, 2203413.

8 Y. Du, L. Zhao, C. Xiong, Z. Sun, S. Liu, C. Li, S. Hao, W. Zhou and H. Li, *Energy Storage Mater.*, 2023, **56**, 310-318.

9 X. Pei, Y. Li, T. Ou, X. Liang, Y. Yang, E. Jia, Y. Tan and S. Guo, *Angew. Chem., Int. Ed.*, 2022, **61**, e202205075.

10 J. Zhang, S. Wang, D. Han, M. Xiao, L. Sun and Y. Meng, *Energy Storage Mater.*, 2020, **24**, 579-587.

11 M. Arrese Igor, M. Martinez Ibañez, E. Pavlenko, M. Forsyth, H. Zhu, M. Armand, F. Aguesse and P. López Aranguren, *ACS Energy Lett.*, 2022, **7**, 1473-1480.

12 S. Ding, J. Chen, X. Deng, Y. Gao, Y. Zhao, X. Kong, Q. Rong, J. Xiong and D. Yu, *Angew. Chem., Int. Ed.*, 2023, **62**, e202307255.

13 W. Liu, C. Yi, L. Li, S. Liu, Q. Gui, D. Ba, Y. Li, D. Peng and J. Liu, *Angew. Chem., Int. Ed.*, 2021, **60**, 12931-12940.

14 Y. F. Huang, T. Gu, G. Rui, P. Shi, W. Fu, L. Chen, X. Liu, J. Zeng, B. Kang, Z. Yan, F. J. Stadler, L. Zhu, F. Kang and Y. B. He, *Energy Environ. Sci.*, 2021, **14**, 6021-6029.

15 R. Lin, Y. He, C. Wang, P. Zou, E. Hu, X. Q. Yang, K. Xu and H. L. Xin, *Nat. Nanotechnol.*, 2022, **17**, 768-776.

16 D. Yu, X. Pan, J. E. Bostwick, C. J. Zanelotti, L. Mu, R. H. Colby, F. Lin and L. A. Madsen, *Adv. Energy Mater.*, 2021, **11**, 2003559.

17 X. He, Y. Ni, Y. Hou, Y. Lu, S. Jin, H. Li, Z. Yan, K. Zhang and J. Chen, *Angew. Chem., Int. Ed.*, 2021, **60**, 22672-22677.

18 T. Deng, X. Ji, Y. Zhao, L. Cao, S. Li, S. Hwang, C. Luo, P. Wang, H. Jia, X. Fan, X. Lu, D. Su, X. Sun, C. Wang and J. G. Zhang, *Adv. Mater.*, 2020, **32**, 2000030.

19. Z. Jiang, S. Wang, X. Chen, W. Yang, X. Yao, X. Hu, Q. Han and H. Wang, *Adv. Mater.*, 2020, **32**, 1906221.

20 N. Hamao, Y. Yamaguchi and K. Hamamoto, *Materials*, 2021, **14**, 4737.

21 S. Kaboli, G. Girard, W. Zhu, A. Gheorghe Nita, A. Vijh, C. George, M. L. Trudeau and A. Paolella, *Chem. Commun.*, 2021, **57**, 11076-11079.

22 W. Weng, D. Zhou, G. Liu, L. Shen, M. Li, X. Chang and X. Yao, *Mater. Futures*, 2022, **1**, 021001.

23 J. S. Kim, G. Yoon, S. Kim, S. Sugata, N. Yashiro, S. Suzuki, M. J. Lee, R. Kim, M. Badding, Z. Song, J. Chang and D. Im, *Nat. Commun.*, 2023, **14**, 782.

24 Y. Song, L. Yang, W. Zhao, Z. Wang, Y. Zhao, Z. Wang, Q. Zhao, H. Liu and F. Pan, *Adv. Energy Mater.*, 2019, **9**, 1900671.

25 D. Wang, L. J. Jhang, R. Kou, M. Liao, S. Zheng, H. Jiang, P. Shi, G. X. Li, K. Meng and D. Wang, *Nat. Commun.*, 2023, **14**, 1895.
26 X. Li, J. Liang, J. Luo, M. Norouzi Banis, C. Wang, W. Li, S. Deng, C. Yu, F. Zhao, Y. Hu, T. K. Sham, L. Zhang, S. Zhao, S. Lu, H. Huang, R. Li, K. R. Adair and X. Sun, *Energy Environ. Sci.*, 2019, **12**, 2665-2671.
27 G. Liu, J. Shi, M. Zhu, W. Weng, L. Shen, J. Yang and X. Yao, *Energy Storage Mater.*, 2021, **38**, 249-254.
28 R. Sahore, B. L. Armstrong, X. Tang, C. Liu, K. Owensby, S. Kalnaus and X. C. Chen, *Adv. Energy Mater.*, 2023, **13**, 2203663.
29 J. Bian, H. Yuan, M. Li, S. Ling, B. Deng, W. Luo, X. Chen, L. Yin, S. Li, L. Kong, R. Zhao, H. Lin, W. Xia, Y. Zhao and Z. Lu, *Front. Chem.*, 2021, **9**, 744417.
30 Y. Nie, T. Yang, D. Luo, Y. Liu, Q. Ma, L. Yang, Y. Yao, R. Huang, Z. Li, E. M. Akinoglu, G. Wen, B. Ren, N. Zhu, M. Li, H. Liao, L. Tan, X. Wang and Z. Chen, *Adv. Energy Mater.*, 2023, **13**, 2204218.
31 P. Didwal, Y. N. Singhbabu, R. Verma, B. Sung, G. H. Lee, J. S. Lee, D. R. Chang and C. J. Park, *Energy Storage Mater.*, 2021, **37**, 476-490.
32 T. Feng, Y. Hu, L. Xu, J. Huang, S. Hu, L. Zhang and L. Luo, *Mater. Today Energy*, 2022, **28**, 101062.
33 X. Ao, X. Wang, J. Tan, S. Zhang, C. Su, L. Dong, M. Tang, Z. Wang, B. Tian and H. Wang, *Nano Energy*, 2021, **79**, 105475.
34 X. Zhou, B. Zhang, F. Huang, F. Li, Z. Ma and J. Liu, *Nano Energy*, 2023, **108**, 108221.
35 S. Chen, Y. Wu, S. Niu, Z. Wei, Y. Wu and W. Wei, *ACS Appl. Energy Mater.*, 2023, **6**, 1989-2000.
36 E. Zhao, Y. Guo, Y. Liu, S. Liu and G. Xu, *Appl. Surf. Sci.*, 2022, **573**, 151489.
37 L. Li, Y. Deng, H. Duan, Y. Qian and G. Chen, *J. Energy Chem.*, 2022, **65**, 319-328.
38 Z. Li, S. Wang, J. Shi, Y. Liu, S. Zheng, H. Zou, Y. Chen, W. Kuang, K. Ding, L. Chen, Y. Lan, Y. Cai and Q. Zheng, *Energy Storage Mater.*, 2022, **47**, 262-270.
39 R. Fan, W. Liao, S. Fan, D. Chen, J. Tang, Y. Yang and C. Liu, *Adv. Sci.*, 2022, **9**, 2104506.
40 Z. Guo, Y. Pang, S. Xia, F. Xu, J. Yang, L. Sun and S. Zheng, *Adv. Sci.*, 2021, **8**, 2100899.
41 P. Shi, J. Ma, M. Liu, S. Guo, Y. Huang, S. Wang, L. Zhang, L. Chen, K. Yang, X. Liu, Y. Li, X. An, D. Zhang, X. Cheng, Q. Li, W. Lv, G. Zhong, Y. B. He and F. Kang, *Nat. Nanotechnol.*, 2023, **18**, 602-610.
42 T. Jiang, P. He, G. Wang, Y. Shen, C. W. Nan and L. Z. Fan, *Adv. Energy Mater.*, 2020, **10**, 1903376.
43 K. Pan, L. Zhang, W. Qian, X. Wu, K. Dong, H. Zhang and S. Zhang, *Adv. Mater.*, 2020, **32**, 2000399.
44 Z. Lin, Y. Wang, Y. Li, Y. Liu, S. Zhong, M. Xie, F. Yan, Z. Zhang, J. Peng, J. Li, A. Wang, X. Chen, M. Zhai, H. Zhang and J. Qiu, *Energy Storage Mater.*, 2022, **53**, 917-926.
45 D. Chen, M. Zhu, P. Kang, T. Zhu, H. Yuan, J. Lan, X. Yang and G. Sui, *Adv. Sci.*, 2022, **9**, 2103663.
46 Z. Wen, Z. Zhao, L. Li, Z. Sun, N. Chen, Y. Li, F. Wu and R. Chen, *Adv. Funct. Mater.*, 2021, **32**, 2109184.
47 Z. Bi, W. Huang, S. Mu, W. Sun, N. Zhao and X. Guo, *Nano Energy*, 2021, **90**, 106498.
48 T. Zhu, G. Liu, D. Chen, J. Chen, P. Qi, J. Sun, X. Gu and S. Zhang, *Energy Storage Mater.*, 2022, **50**, 495-504.
49 Y. Zhai, W. Hou, M. Tao, Z. Wang, Z. Chen, Z. Zeng, X. Liang, P. Paoprasert, Y. Yang, N. Hu and S. Song, *Adv. Mater.*, 2022, **34**, 2205560.
50 C. Wang, H. Liu, Y. Liang, D. Li, X. Zhao, J. Chen, W. Huang, L. Gao and L. Z. Fan, *Adv. Funct. Mater.*, 2022, **33**, 2209828.
51 Y. Wang, S. Chen, Z. Li, C. Peng, Y. Li and W. Feng, *Energy Storage Mater.*, 2022, **45**, 474-483.

52 L. Tang, B. Chen, Z. Zhang, C. Ma, J. Chen, Y. Huang, F. Zhang, Q. Dong, G. Xue, D. Chen, C. Hu, S. Li, Z. Liu, Y. Shen, Q. Chen and L. Chen, *Nat. Commun.*, 2023, **14**, 2301.

53 B. Yang, C. Deng, N. Chen, F. Zhang, K. Hu, B. Gui, L. Zhao, F. Wu and R. Chen, *Adv. Mater.*, 2024, 36, 2403078.

54 S. Kim, H. K. Jung, P. L. Handayani, T. Kim, B. M. Jung and U. H. Choi, *Adv. Funct. Mater.*, 2023, **33**, 2210916.

55 C. Jing, K. Dai, D. Liu, W. Wang, L. Chen, C. Zhang and W. Wei, *Sci. Bull.*, 2024, **69**, 209-217.

56 H. X. Yang, Z. K. Liu, Y. Wang, N. W. Li and L. Yu, *Adv. Funct. Mater.*, 2023, **33**, 2209837.

57 J. Pan, Y. C. Zhang, J. Wang, Z. C. Bai, R. G. Cao, N. N. Wang, S. X. Dou and F. Q. Huang, *Adv. Mater.*, 2022, **34**, 2107183.

58 D. Xu, J. Su, J. Jin, C. Sun, Y. Ruan, C. Chen and Z. Wen, *Adv. Energy Mater.*, 2019, **9**, 1900611.

59 H. Cheng, J. Cao, F. Li, X. Geng, D. Li, Y. Wei, X. Lin, H. Xu and Y. Huang, *Adv. Funct. Mater.*, 2024, **34**, 2307677.

60 K. Mu, D. Wang, W. Dong, Q. Liu, Z. Song, W. Xu, P. Yao, Y. Chen, B. Yang, C. Li, L. Tian, C. Zhu and J. Xu, *Adv. Mater.*, 2023, **35**, 2304686.

61 C. Shen, W. Feng, Y. Yu, H. Wang, Y. Cheng, C. Dong, J. Gu, A. Zheng, X. Liao, X. Xu and L. Mai, *Adv. Energy Mater.*, 2024, **14**, 2304511.